LOW-MULTIPLICITY BURST SEARCH AT THE SUDBURY NEUTRINO OBSERVATORY

B. Aharmim[1], S. N. Ahmed[2], A. E. Anthony[3,19], N. Barros[4], E. W. Beier[5], A. Bellerive[6], B. Beltran[7], M. Bergevin[8,9], S. D. Biller[10], K. Boudjemline[2,6], M. G. Boulay[2], B. Cai[2], Y. D. Chan[9], D. Chauhan[1], M. Chen[2], B. T. Cleveland[10], X. Dai[2,6,10], H. Deng[5], J. Detwiler[9], G. Doucas[10], P.-L. Drouin[6], F. A. Duncan[2,11], M. Dunford[5,20], E. D. Earle[2], S. R. Elliott[12,13], H. C. Evans[2], G. T. Ewan[2], J. Farine[1,6], H. Fergani[10], F. Fleurot[1], R. J. Ford[2,11], J. A. Formaggio[13,14], N. Gagnon[9,10,12,13], J. T. M. Goon[15], K. Graham[2,6], E. Guillian[2], S. Habib[7], R. L. Hahn[16], A. L. Hallin[7], E. D. Hallman[1], P. J. Harvey[2], R. Hazama[13,21], W. J. Heintzelman[5], J. Heise[2,12,17,22], R. L. Helmer[18], A. Hime[12], C. Howard[7], M. Huang[1,3,23], B. Jamieson[17], N. A. Jelley[10], M. Jerkins[3], J. R. Klein[3,5], M. Kos[2], C. Kraus[1,2], C. B. Krauss[7], T. Kutter[15], C. C. M. Kyba[5,24], J. Law[8], K. T. Lesko[9], J. R. Leslie[2], J. C. Loach[9,10], R. MacLellan[2], S. Majerus[10], H. B. Mak[2], J. Maneira[4], R. Martin[2,9], N. McCauley[5,10,25], A. B. McDonald[2], M. L. Miller[13,14], B. Monreal[14,26], J. Monroe[14], B. G. Nickel[8], A. J. Noble[2,6], H. M. O'Keeffe[10,27], N. S. Oblath[13,14], G. D. Orebi Gann[5,10], S. M. Oser[17], R. A. Ott[14], S. J. M. Peeters[10,28], A. W. P. Poon[9], G. Prior[9,20], S. D. Reitzner[8], K. Rielage[12,13], B. C. Robertson[2], R. G. H. Robertson[13], M. H. Schwendener[1], J. A. Secrest[5,29], S. R. Seibert[3,5,12], O. Simard[6], J. J. Simpson[8], D. Sinclair[6,18], P. Skensved[2], T. J. Sonley[14,27], L. C. Stonehill[12,13], G. Tešić[6], N. Tolich[13], T. Tsui[17], R. Van Berg[5], B. A. VanDevender[13,30], C. J. Virtue[1], H. Wan Chan Tseung[10,13], P. J. S. Watson[6], N. West[10], J. F. Wilkerson[13,31], J. R. Wilson[10,32], A. Wright[2], M. Yeh[16], F. Zhang[6], AND K. Zuber[10,33]

(SNO COLLABORATION)

[1] Department of Physics and Astronomy, Laurentian University, Sudbury, Ontario P3E 2C6, Canada
[2] Department of Physics, Queen's University, Kingston, Ontario K7L 3N6, Canada
[3] Department of Physics, University of Texas at Austin, Austin, TX 78712-0264, USA
[4] Laboratório de Instrumentação e Física Experimental de Partículas, Av. Elias Garcia 14, 1°, Lisboa, Portugal
[5] Department of Physics and Astronomy, University of Pennsylvania, Philadelphia, PA 19104-6396, USA
[6] Ottawa-Carleton Institute for Physics, Department of Physics, Carleton University, Ottawa, Ontario K1S 5B6, Canada
[7] Department of Physics, University of Alberta, Edmonton, Alberta T6G 2R3, Canada
[8] Physics Department, University of Guelph, Guelph, Ontario N1G 2W1, Canada
[9] Institute for Nuclear and Particle Astrophysics and Nuclear Science Division, Lawrence Berkeley National Laboratory, Berkeley, CA 94720, USA
[10] Department of Physics, University of Oxford, Denys Wilkinson Building, Keble Road, Oxford OX1 3RH, UK
[11] SNOLAB, Lively, Ontario P3Y 1N2, Canada
[12] Los Alamos National Laboratory, Los Alamos, NM 87545, USA
[13] Center for Experimental Nuclear Physics and Astrophysics, and Department of Physics, University of Washington, Seattle, WA 98195, USA
[14] Laboratory for Nuclear Science, Massachusetts Institute of Technology, Cambridge, MA 02139, USA
[15] Department of Physics and Astronomy, Louisiana State University, Baton Rouge, LA 70803, USA
[16] Chemistry Department, Brookhaven National Laboratory, Upton, NY 11973-5000, USA
[17] Department of Physics and Astronomy, University of British Columbia, Vancouver, BC V6T 1Z1, Canada
[18] TRIUMF, 4004 Wesbrook Mall, Vancouver, BC V6T 2A3, Canada

ABSTRACT

Results are reported from a search for low-multiplicity neutrino bursts in the Sudbury Neutrino Observatory. Such bursts could indicate the detection of a nearby core-collapse supernova explosion. The data were taken from Phase I (1999 November–2001 May), when the detector was filled with heavy water, and Phase II (2001 July–2003 August), when NaCl was added to the target. The search was a blind analysis in which the potential backgrounds were estimated and analysis cuts were developed to eliminate such backgrounds with 90% confidence before the data were examined. The search maintained a greater than 50% detection probability for standard supernovae occurring at a distance of up to 60 kpc for Phase I and up to 70 kpc for Phase II. No low-multiplicity bursts were observed during the data-taking period.

Key words: neutrinos – supernovae: general

Online-only material: color figures

[19] Current address: Center for Astrophysics and Space Astronomy, University of Colorado, Boulder, CO, USA.
[20] Current address: CERN, Geneva, Switzerland.
[21] Current address: Department of Physics, Hiroshima University, Hiroshima, Japan.
[22] Current address: Sanford Laboratory at Homestake, Lead, SD, USA.
[23] Current address: Center of Cosmology and Particle Astrophysics, National Taiwan University, Taipei, Taiwan.
[24] Current address: Institute for Space Sciences, Freie Universität Berlin, Leibniz-Institute of Freshwater Ecology and Inland Fisheries, Germany.

[25] Current address: Department of Physics, University of Liverpool, Liverpool, UK.
[26] Current address: Department of Physics, University of California, Santa Barbara, CA, USA.
[27] Current address: Department of Physics, Queen's University, Kingston, Ontario, Canada.
[28] Current address: Department of Physics and Astronomy, University of Sussex, Brighton, UK.
[29] Current address: Department of Chemistry and Physics, Armstrong Atlantic State University, Savannah, GA, USA.

1. INTRODUCTION

Supernova neutrinos offer unique insights into both the fundamental nature of neutrinos and the complex process of core collapse. Although theoretical calculations predict that a typical supernova releases approximately 3×10^{53} erg of gravitational binding energy, 99% of which is carried away by neutrinos, the only supernova neutrinos ever detected came from a single supernova, SN 1987A (Hirata et al. 1987; Bionta et al. 1987; Alekseev et al. 1987). Many open questions in supernova core-collapse models could be resolved with additional supernova neutrino data, motivating large neutrino detectors to search their data sets for multiple events clustered closely in time, which could be considered candidate supernova neutrino events.

One such neutrino detector, the Sudbury Neutrino Observatory (SNO; Boger et al. 2000), was an imaging water Cerenkov detector located at a depth of 5890 m of water equivalent in the Vale Inco., Ltd. Creighton mine near Sudbury, Ontario, Canada. SNO detected neutrinos using an ultra-pure heavy water (^2H_2O, hereafter D_2O) target contained in a transparent spherical acrylic vessel 12 m in diameter. Neutrino interactions in the vessel produced Cerenkov light that was detected by an array of 9456 photomultiplier tubes (PMTs) supported by a stainless steel geodesic structure. Outside the geodesic structure was 5700 tonnes of light water monitored by outward-facing PMTs in order to identify cosmic-ray muons. The D_2O target allowed SNO to detect neutrino events via three different reactions:

$$\nu_x + e^- \rightarrow \nu_x + e^- \text{ (ES)}$$

$$\nu_e + d \rightarrow p + p + e^- \text{ (CC)}$$

$$\nu_x + d \rightarrow p + n + \nu_x \text{ (NC)}.$$

The neutral current (NC) reaction allowed SNO to detect all active neutrino flavors with equal sensitivity, while the charged current (CC) reaction is exclusive to electron neutrinos. The elastic scattering (ES) reaction is primarily sensitive to electron neutrinos; other flavors can undergo ES reactions but with a smaller cross section. Additionally, SNO could see electron antineutrinos through inverse β decay on deuterium and hydrogen, as well as through elastic scattering:

$$\bar{\nu}_e + d \rightarrow n + n + e^+$$

$$\bar{\nu}_e + p \rightarrow n + e^+$$

$$\bar{\nu}_e + e^- \rightarrow \bar{\nu}_e + e^-.$$

The first reaction can provide a triple coincidence between the two neutrons and the positron, but it has a relatively small cross section. The second reaction has a much higher cross section but occurred only in SNO's 1700 tonnes light water shield, which was between the acrylic vessel and the PMT support structure. For this analysis, we have focused only on the D_2O region.

---

[30] Current address: Pacific Northwest National Laboratory, Richland, WA, USA.
[31] Current address: Department of Physics, University of North Carolina, Chapel Hill, NC, USA.
[32] Current address: Department of Physics, Queen Mary University, London, UK.
[33] Current address: Institut für Kern- und Teilchenphysik, Technische Universität Dresden, Dresden, Germany.

Additional reactions on oxygen isotopes are also possible, but the rarity of ^{17}O and ^{18}O in both the H_2O and D_2O volumes made the event rates from these processes very low.

SNO's sensitivity to all neutrino flavors and the comparison of the rates of the different possible reactions provide exciting opportunities to distinguish various supernova models and investigate neutrino properties (Scholberg 2007; Haxton 2008; Schirato & Fuller 2002). During SNO's run time, it participated in the SuperNova Early Warning System (SNEWS), which was designed to notify the astronomical community within minutes of the detection of a large neutrino burst (Antonioli et al. 2004). In order to avoid triggering on a false burst during this real-time analysis, the threshold for the number of events qualifying as a burst was conservatively set to be 30 events in less than 2 s. Although SNO did not observe such a large burst during its run time, a more thorough search is required to determine whether or not SNO observed any evidence of a supernova.

In this paper, we have searched the SNO data set for low-multiplicity bursts, which we define as bursts of two or more events. Such bursts could come from supernovae in satellites of the Milky Way that are hidden by interstellar dust, from non-standard supernovae in our own Galaxy with relatively low neutrino fluxes or from completely unknown and unexpected sources of neutrinos. The Super-Kamiokande Collaboration has recently published a similar search (Ikeda et al. 2007). Our search is complementary to that of Super-Kamiokande, in that for much of the running period examined here the Super-Kamiokande detector was not operational. Additionally, SNO was primarily sensitive to electron neutrinos, while Super-Kamiokande was primarily sensitive to electron antineutrinos.

2. DATA ANALYSIS

2.1. Data Set

The data analyzed here include two phases of SNO's operation. Phase I ran from 1999 November to 2001 May, and the sensitive volume of the detector was filled only with D_2O. Phase II ran from 2001 July to 2003 August, and during this phase NaCl was added to the detector, increasing the sensitivity to the NC reaction through the consequent enhancement of neutron detection efficiency. Phase II began running shortly after Super-Kamiokande's first phase of data taking ended, meaning that the majority of SNO Phase II contains no overlap with the supernova search performed by Super-Kamiokande. Because of the enhanced NC detection efficiency, SNO Phase II provides a higher sensitivity to a potential supernova signal. The total livetime of Phase I was 241.4 days, while the total livetime of Phase II was 388.4 days. The absolute time of an event was measured by a Global Positioning Satellite system whose accuracy was ~300 ns (Aharmim et al. 2007).

2.2. Search Parameters

We estimated all of the backgrounds that could mimic a supernova burst signal, and we designed our search windows and analysis cuts to ensure that we were 90% confident we would not see a false burst. We optimized our searches by adjusting the minimum burst multiplicity, the length of the coincidence time interval, and the energy threshold for individual events. Our energy threshold sets a lower limit on the reconstructed total energy of the detected electrons, which may have significantly lower energies than the neutrinos themselves. Sensitivity to a supernova signal is increased by selecting a long coincidence

Table 1
Search Windows and Energy Thresholds

Burst Search	Window Length (s)	Energy Threshold (MeV)
Phase I, $N_{event} = 2$	0.05	5.0
Phase I, $N_{event} = 2$	0.2	6.0
Phase I, $N_{event} = 3$	10.0	4.5
Phase II, $N_{event} = 2$	0.05	6.5
Phase II, $N_{event} = 2$	1.0	8.5
Phase II, $N_{event} = 3$	10.0	4.5

Notes. The above values were chosen to maximize our sensitivity while limiting our probability of seeing a false burst. The energy threshold sets a lower limit on the reconstructed total energy of the detected electrons.

time interval, a low-multiplicity requirement, and a low energy threshold, but these criteria must be balanced against the increase in the probability of a "background" burst, especially through accidental coincidences. As the energy threshold is lowered, the event rate goes up, and hence the accidental coincidence rate increases, particularly for low-multiplicity bursts and for a long coincidence time interval. To ensure a 90% probability of seeing no false bursts within a given search window, the expected backgrounds from all sources must sum to no more than 0.11 events. Our optimization ultimately led us to perform three distinct searches: two multiplicity two ($N_{event} = 2$) searches and one multiplicity three ($N_{event} = 3$) searches.

The first of our $N_{event} = 2$ searches used a short window (0.05 s) to focus on detecting neutrinos from a supernova neutronization burst. In the case of a failed supernova, the neutronization burst provides the only potential signal because shortly after the neutronization phase, the supernova collapses into a black hole, abruptly terminating the neutrino signal (Beacom et al. 2000; McLaughlin & Surman 2007; Sumiyoshi et al. 2006). These unusual supernovae are of special interest to astronomers and their neutrino signatures could provide interesting model constraints. The second multiplicity two window was of moderate length (0.2 s for Phase I and 1 s for Phase II) to maximize our sensitivity to a standard supernova event. Table 1 summarizes the search windows and their respective energy thresholds.

The Phase I data set entirely overlaps with the running of Super-Kamiokande, while much of Phase II does not overlap. Consequently, for Phase I our optimization was intended to maintain some neutral current sensitivity, which Super-Kamiokande does not have to great extent, with the aim of being able to detect non-standard burst sources. For Phase II, however, our goal was to maximize overall supernova sensitivity, and therefore we used a fairly large (1 s) search window. The 1 s window required us to raise the energy threshold high enough that there is very little remaining neutral current signal, but it increased our overall sensitivity to standard supernova bursts.

For the multiplicity three search, where accidentals are not a major background, the window for each phase is 10 s and the energy threshold is 4.5 MeV. Primarily because of the low energy threshold available for this search, it provides the best sensitivity to standard supernova bursts.

In order to simulate a "standard" supernova burst, we utilized supernova Monte Carlo simulations based on the Burrows model (Burrows et al. 1992). The average neutrino energies from this

model are $\langle E_{\nu_e} \rangle \simeq 13$ MeV, $\langle E_{\bar{\nu}_e} \rangle \simeq 15.5$ MeV, and $\langle E_{''\nu''_\mu} \rangle \simeq 20$ MeV, where $''\nu''_\mu$ represents any of the flavors ν_μ, $\bar{\nu}_\mu$, ν_τ, or $\bar{\nu}_\tau$ (Thompson et al. 2003).

2.3. Backgrounds

The primary difficulty in performing a triggerless burst search is the elimination of the "background" created by false bursts. In addition to the accidental coincidences, a large number of correlated physics backgrounds must be estimated and almost entirely eliminated. SNO's sensitivity to neutrons makes this problem particularly difficult: any process that produces multiple neutrons can lead to an apparent burst, with the average time between neutron captures being roughly 50 ms in Phase I due to capture on deuterium and 5 ms in Phase II due to capture on Cl. Table 2 shows our background estimates for each of our search windows before we apply any special analysis cuts designed to remove false bursts beyond the standard SNO analysis cuts (Aharmim et al. 2007, 2010). Most of the multiplicity three backgrounds are conservatively assumed to have upper limits corresponding to the multiplicity two estimates.

The dominant correlated backgrounds are interactions by atmospheric neutrinos, which can produce neutrons without any primary large energy deposit to tag the events. For both Phase I and Phase II, the atmospheric background was estimated with the neutrino interaction generator NUANCE (Casper 2002), whose output was then further processed by the full SNO detector simulation. The simulation's atmospheric neutrino energies ranged from 100 MeV to 2 TeV and flavor oscillation corrections were applied. The systematic error in the NUANCE simulation is conservatively estimated to be $\pm 20\%$, and is dominated by uncertainties in the neutrino cross sections.

Most muons traveling through the SNO detector were tagged by outward-looking PMTs, and neutrons following these muons are eliminated by a 20 s software "muon follower" veto. Some muons, however, do not have enough energy to trigger the outward-looking PMTs and will leak into the detector. Fortunately few of these muons are likely to produce multiple neutrons that could mimic a burst. In the entire livetime of Phase II, the effect of the remaining leaked muons is estimated to cause fewer than 1.35 single-neutron events, implying a conservative upper limit of fewer than 0.5 coincidence events for Phase II. Since Phase I would have even fewer coincidences, the same conservative upper limit of 0.5 coincidences is assumed.

Although the SNO detector was constructed from materials with low radioactivity, some radioactive backgrounds still existed, such as ^{238}U, and spontaneous fission from residual radioactivity can lead to false bursts due to multiple neutron capture. Many of the radioactive backgrounds discussed in previous SNO analyses are not significant in this search because they will not produce bursts of events, but fission neutrons from ^{238}U can create a background burst. The amount of ^{238}U in the detector was measured using an inductively coupled plasma mass spectrometer in 2003 September after the addition of NaCl to the heavy water (Aharmim et al. 2004). More ^{238}U could have been present in Phase II than in Phase I because the addition of NaCl prevented the use of SNO's reverse osmosis purification system; therefore, this ^{238}U measurement was used as an upper limit for Phase I. Using the standard probability of a fission producing various neutron multiplicities (Terrell 1957), we estimated a very conservative upper limit of 0.79 (10) fission bursts due to ^{238}U for Phase I (Phase II). This limit also assumed

Table 2
Physics Backgrounds that Could Create False Bursts

Backgrounds	Phase I $N_{event} = 2$ 0.05 s Window	Phase II $N_{event} = 2$ 0.05 s Window	Phase I $N_{event} = 2$ 0.2 s Window	Phase II $N_{event} = 2$ 1 s Window	Phase I $N_{event} = 3$ 10 s Window	Phase II $N_{event} = 3$ 10 s Window
Atmospherics	4.5 ± 0.9	6.9 ± 1.4	1.9 ± 0.4	0.6 ± 0.1	1.5 ± 0.3	7.5 ± 1.5
Muon Spallation	<0.5	<0.5	<0.5	<0.5	<0.5	<0.5
Fission ^{238}U	<0.8	<10	<0.8	<10	<0.8	<3
Photodisintegration	<0.01	0.4 ± 0.03	<0.01	0.4 ± 0.03	<0.01	<0.4
Geo-ν	0.0	0.5 ± 0.1	0.0	0.5 ± 0.1	0.0	<0.5
Reactor-ν	0.02 ± 0.002	1.4 ± 0.3	0.02 ± 0.002	1.4 ± 0.3	<0.02	<1.4
(α, ne^+e^-)	0.02 ± 0.10	0.07 ± 0.07	0.02 ± 0.10	0.07 ± 0.07	<0.02	<0.07
$(n, 2n)$	<0.02	<0.07	<0.02	<0.07	<0.02	<0.07
DSNB	<0.005	<0.005	<0.005	<0.005	<0.005	<0.005
Instrumentals	<0.03	<1	<0.03	<1	<0.03	<1

Notes. Since the search windows have different energy thresholds, we estimate the backgrounds for each search window for both Phase I and Phase II. These backgrounds are further reduced by the analysis cuts described in the text.

a 65% detection efficiency for neutrons above 4.5 MeV and a 40% efficiency for detecting a gamma burst in coincidence with the fission.

A very small fraction of the time, the production of even a single neutron via the NC reaction can lead to an apparent burst. If a γ ray from the capture on deuterium (in Phase I) or chlorine (Phase II) produces an electron above threshold via Compton scattering and then subsequently photodisintegrates a deuteron, it can create a second neutron. Based on the SNO Monte Carlo simulation, this photodisintegration background has been estimated to cause a small background of less than 0.01 coincidences in Phase I and 0.43 ± 0.03 coincidences in Phase II.

Antineutrinos can also lead to apparent bursts, due to the primary positron created in the interaction and the following capture of one or two neutrons. Antineutrinos from radioactive nuclei in the Earth surrounding the detector lead to a negligible background from this process for Phase I and 0.5 ± 0.1 bursts for Phase II. A study of all commercial nuclear reactors within 500 km of SNO determined that the coincidence background from antineutrinos from these reactors was also very small, 0.019 ± 0.002 coincidences for Phase I and 1.4 ± 0.3 for Phase II.

During the SNO detector construction, the acrylic was exposed to air containing radon. In the decay chain of radon is ^{210}Po, which can decay via α-emission. The α can interact with the carbon in the acrylic, leading to ^{13}C$(\alpha, n)^{16}$O reactions in which the ^{16}O will produce an e^+e^- pair or a γ-ray that can photodisintegrate deuterium. The estimates of (α, n) coincidences from Monte Carlo studies of this background are low. Coincidences due to the diffuse supernova background (DSNB) and to instrumental background events are also estimated to be quite low, as shown in Table 2.

2.4. Analysis Cuts

We developed a set of analysis cuts, beyond the standard cuts used by other SNO analyses (Aharmim et al. 2010, 2007), to reduce the level of correlated backgrounds shown in Table 2 and discussed in the previous section. As in previous analyses, we utilized a fiducial volume radius of 550 cm, as well as a variety of instrumental cuts based on PMT charge and timing information. Our high level cuts incorporated information such as the isotropy of the detected light and the event's reconstruction quality, but we did not include any of the cuts SNO previously designed to remove bursts from the data set. Instead we designed new cuts

that could discriminate between background bursts and potential supernova bursts.

False bursts from atmospheric reactions often have a high-energy primary, followed by delayed neutron captures. We removed these bursts by imposing a deadtime window following any event whose energy exceeded roughly 80 MeV. The 80 MeV threshold was chosen to minimize the acceptance loss for neutrinos from a standard supernova, whose energies tend to peak near 20 MeV. For Phase I, in which the neutron capture time is ∼50 ms, we used a deadtime window of 600 ms, and for Phase II, in which the capture time is ∼5 ms, we used a deadtime window of 200 ms. When we applied this cut to our Monte Carlo simulation of a standard supernova, no genuine supernova bursts were removed.

In addition to having large energies, the primaries from an atmospheric neutrino interaction often have multiple tracks or are heavier particles than the electrons expected either from charged current supernova interactions or from the Compton scattering of γ rays released in neutron capture. We removed false bursts associated with these events by tagging any event that was not electron-like, and removing all events within 600 ms (Phase I) and 200 ms (Phase II) afterward. Our definition of an electron-like event was based on the PMT hit pattern and Kolmogorov–Smirnov tests on the angular distribution of Cerenkov light of reconstructed events, as has been done in other SNO analyses (Aharmim et al. 2010). We estimated the acceptance of this cut by applying it to our Monte Carlo simulation of supernova bursts, and we found that for both phases of the experiment, only 1.2% of genuine supernova bursts were removed. The same cut applied to simulated atmospheric neutrino events removed 57% of those bursts that pass the standard analysis cuts from Phase I and 63% from Phase II.

With the exception of accidental coincidences, almost all sources of false bursts are spatially correlated. Neutrons from atmospheric interactions or fission will capture near the primary event and near one another. To remove events on this basis, we use a cut developed by the Super-Kamiokande Collaboration in their triggerless burst analysis (Ikeda et al. 2007). We define Δr as a weighted mean of the distances between the reconstructed event positions in a candidate burst:

$$\Delta r = \frac{\sum_{i=1}^{M-1} \sum_{j=i+1}^{M} |\vec{r}_i - \vec{r}_j|}{{}_M C_2}, \quad (1)$$
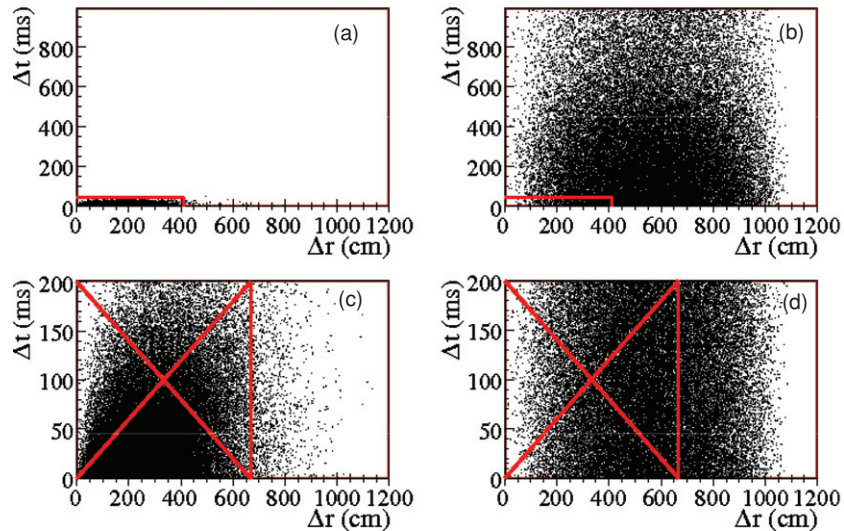
Figure 1. (a) Simulated background bursts in the 1 s search window for Phase II: the region inside the box was removed by the $\Delta r \Delta t$ cut, which eliminates most of the background events. (b) Simulated supernova signal in the 1 s window for Phase II: the $\Delta r \Delta t$ cut removes very little of the simulated signal. (c) Simulated background bursts in the 0.2 s search window for Phase I: the region marked with an "X" was removed by the Δr cut, which eliminates most of the background events. (d) Simulated supernova signal in the 0.2 s search window for Phase I: the Δr cut must remove a large fraction of the supernova signal in order to sufficiently eliminate background bursts.

(A color version of this figure is available in the online journal.)

Table 3
Fraction of Standard SN Signal that Survives the $\Delta r \Delta t$ Cut

Burst Search	Δr Cut (cm)	Δt Cut (ms)	α_1 (ms)	α_2 (ms)^2/(cm)	α_3 (cm)	SN Signal
Phase I, 0.05 s window	626	...	...	...	...	0.389
Phase I, 0.2 s window	668	...	...	...	...	0.303
Phase I, 10 s window	600	180	180	100	376	0.867
Phase II, 0.05 s window	385	40	40	5	200	0.811
Phase II, 1 s window	410	45	...	...	...	0.977
Phase II, 10 s window	400	35	35	10	300	0.999

Notes. Only the Δr cut was applied to the $N_{\mathrm{event}} = 2$ searches in Phase I, while we applied the $\Delta r \Delta t$ cut to Phase II and to the $N_{\mathrm{event}} = 3$ search in Phase I. The $\Delta r \Delta t$ cuts were generally box-shaped with one rounded corner described by the α parameters.

Table 4
Low-multiplicity Bursts in the Background-contaminated Region

Search Description	Bursts Expected in $\Delta r \Delta t$ Excluded Region	Bursts Found in $\Delta r \Delta t$ Excluded Region
Phase I, 0.05 s window	4.53 ± 0.91	2
Phase I, 0.2 s window	1.90 ± 0.38	1
Phase I, 10 s window	1.51 ± 0.30	2
Phase II, 0.05 s window	6.94 ± 1.39	7
Phase II, 1 s window	0.57 ± 0.11	1
Phase II, 10 s window	7.51 ± 1.50	9

where $|\vec{r_i} - \vec{r_j}|$ is the distance between the reconstructed positions of events i and j within a burst, M is the multiplicity of the burst, and $_M C_2$ is the number of non-redundant combinations. For SNO, we can improve on the straightforward Δr cut by using the fact that most spatially correlated events are due to neutron captures, and therefore there is a direct relationship between Δr of the events and the time that separates them, due to the neutron diffusion time within the heavy water. We therefore examined not just the spatial separation of burst events but also their separation in time, Δt, which is defined similarly to Equation (1). Figure 1 shows a $\Delta r \Delta t$ distribution for $N_{\mathrm{event}} = 2$ from Phase II where the two-dimensional cut is clearly beneficial. The figure also shows the same distribution for Phase I, where the longer neutron capture time and longer diffusion distance makes the two-dimensional cut less effective and hence we use only the cut on Δr. For both phases, we applied the two-dimensional cut to the $N_{\mathrm{event}} = 3$ search. Table 3 summarizes the fraction of expected supernova signal that survives the Δr or $\Delta r \Delta t$ cut for each of the search windows. The functional form of the $\Delta r \Delta t$ cut was generally box-shaped, though for several of the search windows the shape of the cut included a rounded corner described by $\Delta t > \sqrt{\alpha_1^2 + \alpha_2 \alpha_3 - \alpha_2 \Delta r}$. Table 3 shows the parameter

values used for the $\Delta r \Delta t$ cut for each of the search windows. In Phase I, the long diffusion distance makes eliminating backgrounds more difficult, meaning that the Δr cut must be harsher in order to adequately reduce the probability of seeing a false burst.

3. RESULTS

After estimating all of the background sources of false bursts that could mimic a supernova burst signal, we placed our analysis cuts to ensure that we expected no more than 0.11 events in each search window. Our approach to the low-multiplicity search was inherently blind: we did not examine the real data until we had set all of our search parameters, and we did not change any of those parameters after we performed the search.

Our $\Delta r \Delta t$ cut defined an "antibox" region that was excluded from the supernova burst search, as shown in Figure 1. Prior to opening the box and examining the events passing the analysis cuts, we examined the antibox in order to confirm our estimates of background bursts. We found approximately the same number of bursts there that we expected, as shown in Table 4. Because our background was dominated by atmospheric neutrino bursts and several of our other background estimates were conservative upper limits, Table 4 compares the number of bursts we observed outside the box to the number of bursts we expected due to atmospheric events.
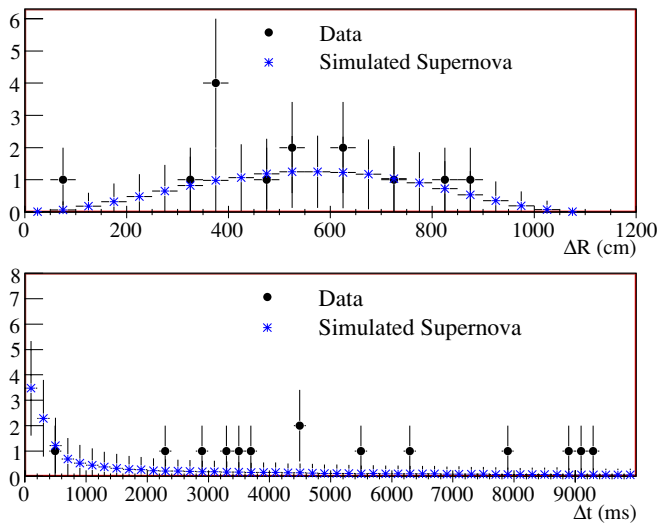
Figure 2. Δr and Δt distributions for $N_{event} = 2$ bursts found in the $N_{event} = 3$ search window for Phase II. These bursts are consistent with expected accidental coincidences and are not considered candidate supernova bursts.

(A color version of this figure is available in the online journal.)

Table 5
Low-multiplicity Bursts Found in the SNO Data Set

Search Description	Bursts Expected in Search Region	Bursts Found in Search Region
Phase I, 0.05 s window	<0.11	0
Phase I, 0.2 s window	<0.11	0
Phase I, 10 s window	<0.11	0
Phase II, 0.05 s window	<0.11	0
Phase II, 1 s window	<0.11	0
Phase II, 10 s window	<0.05	0

Note. We observed no candidate bursts in any of the search windows.

After all the cuts were developed and tested on simulations, we fixed our analysis and performed our burst searches on both the Phase I and Phase II data. We observed no bursts in any of our search windows, as summarized in Table 5.

Because our 10 s window search was optimized for an $N_{event} = 3$ burst, we did observe some $N_{event} = 2$ bursts in that window. Using the same energy threshold and analysis cuts designed for the Phase II 10 s $N_{event} = 3$ search, we observed 14 $N_{event} = 2$ bursts, which is in keeping with our expectations from accidental coincidences. Figure 2 shows the distribution of Δr and Δt for these $N_{event} = 2$ bursts. The distribution in Δr is approximately uniform, which is consistent with the hypothesis that these are accidental bursts, though it is also consistent with the hypothesis that these are supernova bursts. The Δt distribution supports the conclusion that these are accidental bursts since the events are spread evenly throughout the time window, in contrast with our expectations from an actual supernova. The event with the lowest Δt separation also has a Δr too low to have survived any of the $\Delta r \Delta t$ cuts for the multiplicity two searches, meaning that it is more likely to have been a background burst than a genuine supernova burst. We also observed two $N_{event} = 2$ bursts in the $N_{event} = 3$ search for Phase I. These two bursts are separated by 3.2 s and 8.0 s, respectively, which puts them well outside of the $N_{event} = 2$ search windows. These bursts are also consistent with our accidental coincidence expectations.
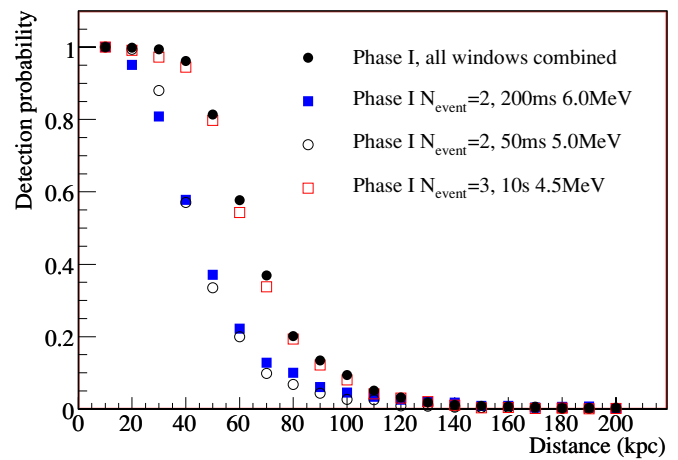

Figure 3. Probability of detecting a supernova in Phase I data assuming a standard Burrows model.

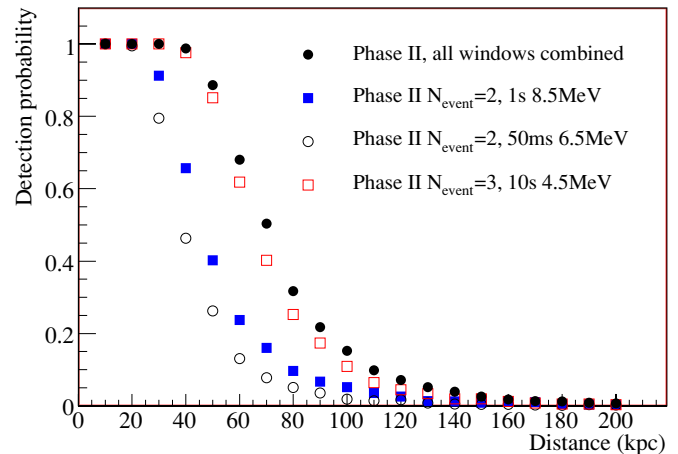(A color version of this figure is available in the online journal.)

Figure 4. Probability of detecting a supernova in Phase II data assuming a standard Burrows model.

(A color version of this figure is available in the online journal.)

4. DISCUSSION AND CONCLUSIONS

We performed a triggerless search for low-multiplicity bursts in data from Phase I (D_2O only) and Phase II (D_2O loaded with NaCl) of the SNO, finding no candidate bursts. For the period of overlap our results are consistent with the null signal observed by Super-Kamiokande.

Figures 3 and 4 show the sensitivity of our various search windows to a standard supernova for both phases as a function of supernova distance. These figures do not include the small dispersion effects arising from the nonzero mass of the neutrino. For Phase I, which was completely overlapped by the run time of Super-Kamiokande, our search was primarily looking for non-standard supernova signals in which ν_e emission would be suppressed, allowing SNO to detect a neutral current signal that Super Kamiokande might not have seen.

At a typical distance in our Galaxy, 10 kpc, we retain a 100% detection probability for a standard core-collapse supernova. In Phase I, we maintain a 50% detection probability for a standard supernova out to 60 kpc. In Phase II, we retain a 100% detection probability out to 30 kpc and a greater than 50% detection probability out to 70 kpc.

REFERENCES

Aharmim, B., et al. (SNO Collaboration) 2004, Phys. Rev. D, 70, 093014
Aharmim, B., et al. (SNO Collaboration) 2007, Phys. Rev. C, 75, 045502
Aharmim, B., et al. (SNO Collaboration) 2010, Phys. Rev. C, 81, 055504
Alekseev, E. N., Alekseeva, L. N., Volchenko, V. I., & Krivosh, I. V. 1987, J. Exp. Theor. Phys. Lett., 45, 589
Antonioli, P., et al. 2004, New J. Phys., 6, 114
Beacom, J. F., Boyd, R. N., & Mezzacappa, A. 2000, Phys. Rev. Lett., 85, 3568
Bionta, R. M., Blewitt, G., Bratton, C. B., Casper, D., & Ciocio, A. 1987, Phys. Rev. Lett., 58, 1494
Boger, J., et al. 2000, Nucl. Instrum. Methods Phys. Res. A, 449, 172
Burrows, A., Klein, D., & Gandhi, R. 1992, Phys. Rev. D, 45, 3361
Casper, D. 2002, Nucl. Phys. B: Proc. Suppl., 112, 161
Haxton, W. C. 2008, in Encyclopedia of Applied High Energy and Particle Physics, 221, ed. R. Stock (Weinheim: Wiley-VCH Verlag GmbH & Co.), arXiv:0808.0735
Hirata, K. S., Kajita, T., Koshiba, M., Nakahata, M., & Oyama, Y. 1987, Phys. Rev. Lett., 58, 1490
Ikeda, M., et al. 2007, ApJ, 669, 519
McLaughlin, G. C., & Surman, R. 2007, Phys. Rev. D, 75, 023005
Schirato, R. C., & Fuller, G. M. 2002, arXiv:astro-ph/0205390
Scholberg, K. 2007, arXiv:astro-ph/0701081
Sumiyoshi, K., Yamada, S., Suzuki, H., & Chiba, S. 2006, Phys. Rev. Lett., 97, 091101
Terrell, J. 1957, Phys. Rev., 108, 783
Thompson, T. A., Burrows, A., & Pinto, P. A. 2003, ApJ, 592, 434